An in-vitro evaluation of the polo-like kinase inhibitor GW843682X against paediatric malignancies

Kristina Spaniol, Joachim Boos and Claudia Lanvers-Kaminsky

Polo-like kinase 1 (PLK1) is a regulator of mitosis and its upregulation in tumours is often associated with poor prognosis. Although PLK1 inhibitors have already entered phase 1 clinical trials, little is known about their impact on the treatment of paediatric malignancies. Thus, we evaluated the concept of PKL1 inhibition by testing the effects of the PLK1 inhibitor GW843682X alone and in combination with the topoisomerase 1 inhibitor, camptothecin, against a panel of 18 paediatric tumour cell lines. Cytotoxicity was evaluated by MTT test and by caspase 3/7 activation. Expression of target was confirmed by western blot analysis. Expression of ATP binding cassette transporters was analysed by quantitative real-time reverse transcription PCR. GW843682X significantly inhibited cell growth in all 18 cell lines. Concentrations, which inhibited cell growth by 50% compared with untreated controls after 72 h, ranged from 0.02 to 11.7 μmol/l. Apart from the N-Myc-amplified neuroblastoma cell lines, the osteosarcoma cell lines MNNG-HOS and OST, which are highly resistant to standard anticancer drugs, were sensitive to GW843682X. The toxicity of GW843682X was dependent neither on the ATP binding cassette drug transporter expression nor on the p53 mutation status. Neither synergistic nor antagonistic effects were observed for the combination of GW843682X and camptothecin in 14 cell lines. GW843682X showed considerable toxicity against a panel of paediatric tumour cell lines suggesting that PLK1 inhibitors under clinical development should be evaluated against paediatric malignancies too. *Anti-Cancer Drugs* 22:531–542 © 2011 Wolters Kluwer Health | Lippincott Williams & Wilkins.

Anti-Cancer Drugs 2011, **22**:531–542

Keywords: camptothecin, GW843682X, paediatric malignancies, polo-like kinase 1

Department of Paediatric Haematology and Oncology, University Children's Hospital, Muenster, Germany

Correspondence to Claudia Lanvers-Kaminsky, PhD, Department of Paediatric Haematology and Oncology, University Children's Hospital, Albert Schweitzer Strasse 33, D-48149 Muenster, Germany
Tel: +49 251 8355693; fax: +49 251 8355740;
e-mail: lanvers@uni-muenster.de

Received 15 October 2010 **Revised form accepted** 1 February 2011

Introduction

Despite all efforts, the prognosis of children with advanced-staged malignancies still remains poor. During the search for new and more selective anticancer drugs, polo-like kinase 1 (PLK1) has emerged as a promising target. PLK1 is a key regulator of mitotic progression and G2–M transition [1]. It promotes mitotic progress such as mitotic entry, centrosome maturation, spindle assembly, anaphase-promoting complex/C regulation and cytokinesis [2]. Overexpression of PLK1 has been observed not only in numerous tumour types such as cancer of the breast, ovary, colon, pancreas, lung, endometrium, brain, skin, head and neck, gastric tract, prostate and oesophagus but also has been associated with poor prognosis [3]. Furthermore, depletion of PLK1 activity induced apoptosis in tumour cells [4,5], whereas nonmalignant cells were not affected [6].

Non-ATP-competitive as well as ATP-competitive small molecule inhibitors of PLK1 were developed, and recently BI 2536, a small molecule ATP-competitive inhibitor of PLK1, has entered phase 1 clinical trials in adults [7,8]. As only limited data are available so far on the use of PLK1 inhibition against paediatric malignancies [9], we studied the concept of PLK1 inhibition against paediatric malignancies by screening the toxicity of the publicly available PLK1 inhibitor, GW843682X, against a panel of 18 permanent tumour cell lines. Along with GW843682X, we evaluated the effects of the topoisomerase I inhibitor, camptothecin (CPT), combined with GW843682X in a constant ratio of 1 : 1.

Materials and methods

Cell culture

The cytostatic and cytotoxic effects of GW843682X, the topoisomerase 1 inhibitor, CPT and other standard anticancer drugs were tested on a panel of 18 permanent human tumour cell lines comprising four Ewing sarcoma (EWS) cell lines (CADO-ES-1, STA-ET-1, STA-ET-2.1, VH-64), four neuroblastoma (NB) cell lines (IMR5, SMS-KCN, SHEP, SH-SY5Y), two medulloblastoma (MB) cell lines (DAOY, UW228.2), two rhabdomyosarcoma (RMS) cell lines (RD, RH30), two osteosarcoma (OS) cell lines (MNNG-HOS, OST), two human T-ALL cell lines (CCRF-CEM, MOLT-4), the human B-cell precursor ALL cell line (REH) and the human acute myeloid leukaemia cell line (HL-60). Table 1 summarizes the cell line sources and main characteristics. All cell lines represent tumours that typically occur in children and adolescents, and except for the HL-60 cell line, all cell lines were established from tumours of children

0959-4973 © 2011 Wolters Kluwer Health | Lippincott Williams & Wilkins DOI: 10.1097/CAD.0b013e3283454526

Table 1 Cell line characteristics

Tumor type	Cell lines	Description	p53	References
Ewing sarcoma	CADO-ES-1	Established from the malignant pleural effusion from a 19-year-old Japanese woman diagnosed with right-buttock Ewing's sarcoma with multiple lung metastasis, translocation *t*(21,22), fusion transcript EWS/ERG;	wt	[10–12]
	STA-ET-1	Established from a pPNET of the humerus of a 13-year-old girl: translocation *t*(11,22) (q24;q12);	wt	[12,13]
	STA-ET-2.1	Established from a pPNET of the fibula of a 15-year-old boy; translocation *t*(11,22), EWS/FLI1 fusion, p53 mutation, del(22)(q12);	mu	[12,13]
	VH-64	Established from the malignant pleural effusion from a 24-year-old man diagnosed with Ewing's sarcoma of the metatarsus with multiple lung metastasis, translocation *t*(11,22) (q24;q12), fusion transcript EWS/FLI1;	wt	[12,14]
Leukaemia	CCRF-CEM	Established from the peripheral blood of a 3-year-old Caucasian girl with relapsed T-ALL;	mu	[15–18]
	HL-60	Established from the peripheral blood of a 35-year-old woman AML-M2	mu	[18–22]
	MOLT-4	Established from the peripheral blood of a 19-year-old man with relapsed acute lymphoblastic T cell leukaemia	mu	[18,23,24]
	REH	Established from the peripheral blood of a 15-year-old North African girl with precursor B-lineage ALL with TEL/AML1 fusion at first relapse	mu	[18,25]
Medulloblastoma	DAOY	Established from biopsy material taken from a tumour in the posterior fossa of a 4-year-old boy, hypertetraploid, original tumour with characteristics of neuronal and glial differentiation, which were not retained by the cell line	mu	[26–29]
	UW228.2	Established from a posterior fossa medulloblastoma of a 9-year-old female	–	[30]
Neuroblastoma	IMR-5	Subclone of the IMR-32 cell line, which was derived from an abdominal mass diagnosed as neuroblastoma of a 1-year-old Caucasian boy; N-Myc amplified (50-100 copies), 1p deletion	wt	[31–34]
	SMS-KCN	Established from a neuroblastoma of a boy, 1p deletion, N-Myc amplification (100 copies)	wt	[35,36]
	SHEP	Subclone of the SK-N-SH cell line that had been established from the bone marrow biopsy of a 4-year-old girl with metastatic neuroblastoma, no N-Myc amplification, no 1p deletion	wt	[37–41]
	SH-SY5Y	Thrice cloned subline of the SK-N-SH cell line (SK-N-SH: established from bone marrow metastasis of a 4-year-old girl with neuroblastoma); no 1p deletion and no N-Myc amplification	wt	[37–41]
Osteosarcoma	MNNG-HOS	Chemically transformed cell line derived from an osteosarcoma of a 13-year-old female	mu	[12,42–44]
	OST	Established from an osteoblastic osteosarcoma in the diaphysis of the left femur of a 15-year-old girl	wt	[45–47]
Rhabdomyosarcoma	RD	Established from embryonal rhabdomyosarcoma of the pelvis in a 7-year-old Caucasian female	mu	[48–51]
	RH-30	Established from the bone marrow metastasis of a 17-year-old man with undifferentiated (standard classification) or unclassified (Palmer classification) alveolar rhabdomyosarcoma; high levels of both myogenin and myoD, expression of Pax3/FKHR fusion protein secondary to the *t*(2;13)(q35;q14) translocation	wt	[51–54]

'–', unknown; ERG, Ets-related gene; mu, mutated; pPNET, peripheral primitive neuroectodermal tumour; wt, wild type; EWS, Ewing sarcoma.

or adolescents. CCRF-CEM, MOLT-4, REH, HL-60, CADO-ES-1, SH-SY5Y, SAOS-2 and RH-30 were purchased from the German Collection of Microorganisms and Cell Cultures (DSMZ, Braunschweig, Germany). DAOY, RD, MG-63, U-2OS, MNNG-HOS and IMR-5 were acquired from ATCC-LGC (Promochem GmbH, Wesel, Germany). SMS-KCN, SHEP and OST were kindly provided by Professor C. Poremba (Institute of Pathology, University of Duesseldorf, Germany). UW228.2 was allocated by Professor Michael Frühwald (Department of Paediatric Haematology and Oncology, University Children's Hospital Muenster, Muenster, Germany) with the kind permission of Professor John Silber (Department of Neurological Surgery, University of Washington, Washington, Seattle, USA). Finally, STA-ET-1, STA-ET-2.1 and VH-64 were kindly provided by F. van Valen (Department of Orthopaedics, University Hospital Muenster, Muenster, Germany). All cell lines were grown in RPMI 1640 medium supplemented with 2 mmol/l L-glutamine, 10% foetal bovine serum, 10^5 U/l penicillin, 100 mg/l streptomycin and 25 mg/l amphotericin B (GibcoBRL cell culture, Invitrogen GmbH, Karlsruhe, Germany). Tissue culture flasks were incubated in a humidified atmosphere of 5% CO_2 at 37°C. The EWSs were grown in tissue culture flasks coated with collagen. At regular intervals, all cell lines were screened for mycoplasma infection. In addition, all cell lines were subjected to short tandem repeat analysis using the AmpFlSTR Identifiler PCR Amplification kit (Applied Biosystems, Applera Deutschland GmbH, Darmstadt, Germany) according to the manufacturer's instruction.

Cytotoxicity assays

Cell viability was measured by the MTT test, as described earlier [55]. Depending on the doubling time, 3000 or 5000 cells per well were seeded in 96-well plates and incubated for 72 h. GW843682X and CPT were solubilized in dimethyl sulfoxide at concentrations of 5 mg/ml for GW843682X and 50 mg/ml for CPT.

Dilutions for GW843682X, CPT and a combination of both drugs were prepared in complete cell culture medium by serial log dilutions. Final test concentrations were 100, 10, 1, 0.1, 0.01, 0.001 and 0.0001 μmol/l for

GW843682X and CPT. After 72 h, the viability of each cell population at the day of drug addition (day 0) was analysed by the MTT test. The remaining plates were inoculated with 100 µl of the respective drug dilutions resulting in a final volume of 200 µl; control cells were inoculated with medium only. The cells were incubated for another 72 h and thereafter analysed for cell viability by the MTT test. MTT is reduced to violet formazan by vital and early apoptotic cells. The formation of blue formazan dye was quantified at a wavelength of 560 nm and a reference wavelength of 650 nm using an Elisa reader (Multiscan Ascent, Thermo Scientific, Langenselbold, Germany).

In each experiment, each drug concentration was tested in quadruplate and each experiment was repeated independently three times. Experiments were considered valid only when the cells proliferated within the range of their characteristic population doubling times. Within each experiment, the coefficients of variation of at least three out of four measurements were below 15% and the coefficient of variation of cell viability determined for each drug concentration and cell line from three individual experiments was below 20%.

Calculation of cell viability

In each individual experiment for each test concentration, means and standard deviations were calculated from quadruplate. Out of these mean optical density (OD) values, the rate of cell viability was calculated (i) by comparing the rate of cell viability of treated cells with that of untreated cells at the end of the experiment (72 h) [equation 1: (mean OD of treated wells at 72 h/mean ODs of untreated wells at 72 h) × 100%] and (ii) by comparing the cell viability of treated cells with that of untreated cells at the start of the experiment (0 h) [equation 2: (mean OD of treated wells at 72 h/mean ODs of untreated wells at 0 h) × 100%].

For the determination of the half maximal growth inhibitory concentration (GI_{50}) value, which is the drug concentration needed to reduce cell growth by 50% compared with untreated controls at the end of the incubation (72 h), the rate of cell viability determined by equation (1) was used to calculate the GI_{50} according to the following equation: $GI_{50} = 50\% \times [(\text{drug concentration above } 50\% \text{ cell survival}) - (\text{drug concentration below } 50\% \text{ cell survival})]/[(\%\ \text{cell survival} > 50\%) - (\%\ \text{cell survival} < 50\%)]$.

For calculations of the lethal concentration (LC_{50}) value, which is the drug concentration needed to kill 50% of the cells compared with the start of drug exposure (0 h), the rate of cell viability determined by equation (2) was used to calculate the LC_{50} according to the following equation: $LC_{50} = 50\% \times [(\text{drug concentration above } 50\% \text{ cell survival}) - (\text{drug concentration below } 50\% \text{ cell survival})]/[(\%\ \text{cell survival} > 50\%) - (\%\ \text{cell survival} < 50\%)]$.

For each cell line and each experiment, the calculated GI_{50s} and LC_{50s} were log-transformed. Out of the log-transformed GI_{50s} or LC_{50s} of all experiments, means were calculated and the log-transformed GI_{50s} or LC_{50s} of the individual experiments were subtracted from the respective means. For cell lines that reacted more sensitively to the test drug compared with the other cell lines of the cell line panel, positive values were scheduled, whereas negative differences identified the more resistant cell lines within the cell line panel. For the leukaemia cell lines HL-60 and REH, the LC_{50s} did not reach the highest concentration of CPT and GW843682X tested. For the calculation of differences of mean, the LC_{50s} of these experiments were set to 100 µmol/l. As the actual LC_{50s} for REH and HL-60 were greater than 100 µmol/l, the calculated means for CPT and GW843682X were faintly underestimated and consequently the difference of mean for the single experiments too.

Western blot

Total lysates were prepared in the presence of protease inhibitors with lysis buffer (radioimmunoprecipitation assay buffer: 150 mmol/l NaCl, 0.5% sodium deoxycholate, 50 mmol/l Tris–HCl, 0.1% SDS, 1% NP-40) supplemented with the Complete Protease Inhibitor Cocktail (Roche Diagnostics, Mannheim, Germany). The protein content of lysates was determined using the BCA protein assay kit (Thermo Scientific). Total protein (50 µg) was loaded onto a 7.5% gel, electrophoresed in a Bio-Rad Mini-PROTEAN Treta Cell (Bio-Rad, Munich, Germany), and then transferred to a polyvinylidene fluoride transfer membrane (Thermo Scientific). The membrane was blocked by incubation with 3% dry milk in PBS buffer for 60 min at 37°C, probed overnight at 4°C with the 1 : 1000 diluted PLK1 antibody (Millipore, Schwalbach, Germany) and then with horseradish peroxidase-conjugated donkey anti-rabbit immunoglobulin G (Millipore) at a dilution of 1 : 10 000. Immunoreactive bands were detected using the Immobilon Western Chemiluminescent Horseradish peroxidase Substrate (Millipore), and recorded and analysed using the Decon Chemoluminescence DeVision HQ along with the chemiluminescence analysis software (Decon Science Tec GmbH, Hohengandern, Germany).

ATP binding cassette-transporter mRNA expression

Total RNA was isolated from cell lines using the QIAamp RNA isolation kit (Qiagen, Hilden Germany) according to the manufacturer's instructions. Trace amounts of DNA were digested on column during RNA purification using the RNase-Free DNase Set (Qiagen). RNA quality and quantity were analysed with the 2100-Bioanalyzer (Agilent Technologies, Waldbronn, Germany). The RNA integrity number of the RNA samples ranged from 8.0 to 10.0. Oligo-dT primed reverse transcription was performed with the Superscript III First-Strand Synthesis System for real-time reverse transcription (RT-PCR)

(Invitrogen GmbH) using 0.5 μg of RNA. RT-PCR for ATP binding cassette B1 (*ABCB1*), *ABCC1*, *ABCC2*, *ABCC3*, *ABCC5*, *ABCC6* and *ABCG2* genes was carried out by the ABI Prism 7700 sequence detection system (Applied Biosystems) with commercially available FAM-labelled probes and primers from Applied Biosystems (Hs0106 7802_m1 for *ABCB1*, Hs00219905_m1 for *ABCC1*, Hs00 166123_m1 for *ABCC2*, Hs00358656_m1 for *ABCC3*, Hs00981089_m1 for *ABCC5*, Hs01081201_m1 for *ABCC6*, Hs01053790_m1 for *ABCG2*). For all RT-PCR assays, 10 ng of total cDNA was used. Assays were run with 2 × Universal PCR Master Mix without uracil-*N*-glycosylase using the following cycling conditions: 10 min at 95°C, 15 s at 95°C, 1 min at 60°C and 40 cycles. The PCR set-up was carried out by a Tecan Genesis 150 robotic (Tecan Deutschland GmbH, Crailsheim, Germany) on a 384-well plate. For normalization, the housekeeping gene glyceraldehyde 3-phosphate dehydrogenase was selected. Data were collected and analysed with the sequence detector software (SDS2.2, Applied Biosystems). Analysis of the relative quantity gene expression data was carried out using the $2^{-[\Delta\Delta]Ct}$ method. Each cell line was analysed in triplicate for target mRNA expression.

Analysis of caspase activation

Caspase activation was determined using the caspase-Glo 3/7 assay supplied by Promega (Mannheim, Germany) according to the manufacturer's instructions. Cells (5×10^4 cells/well) were seeded in white-walled 96-well plates (Greiner, Greiner Bio-One GmbH, Solingen, Germany) treated with GW843682X as indicated. Luminescence was measured with the Fluoroskan Ascent FL (Thermo Scientifics).

Statistical analysis

Statistical analysis was carried out using the Sigma Stat 3.2 software (SPSS GmbH Software, Munich, Germany). Correlation analyses were carried out by Pearson product moment correlation for continuous variables and by Spearman rank-order correlation for categorized variables. Results were considered significant when *P* value was less than 0.05.

Results

GW843682X effectively reduced the growth of all 18 tumour cell lines tested. The GI_{50s} ranged from 0.02 μmol/l for the leukaemia cell line, CCRF-CEM, to 11.7 μmol/l for the MB cell line, UW228.2. Apart from UW228.2, the EWS cell line, CADO-ES-1, the NB cell line, SHEP, and the RMS cell lines, RD and RH-30, showed a more resistant phenotype, whereas the leukaemia cell lines, CCRF-CEM and MOLT-4, were sensitive to the growth inhibitory effects of GW843682X (Fig. 1a). The GI_{50s} of the remaining cell lines scattered around the mean GI_{50} and these cell lines were considered intermediately sensitive to GW843682X. Within the cell line panel, the lowest LC_{50} of GW843682X, which resulted in a net loss of 50% cell viability, was determined for the leukaemia cell line, CCRF-CEM ($LC_{50-CCRF-CEM}$: 0.64 μmol/l). For the leukaemia cell lines, REH and HL-60, no reduction of cell viability by 50% compared with the start of the experiment was observed at the highest test concentration used ($LC_{50} > 100$ μmol/l). With regard to the cytotoxicity of GW843682X within this panel of cell lines, two of two OS cell lines, three of four NB cell lines, two of four leukaemia cell lines, one of two RMS cell lines, one of four EWS and no MB cell line showed a sensitive phenotype (Fig. 1b). PLK1 protein expression was detected in all 18 cell lines (Fig. 2). Apart from the leukaemic cell line, CCRF-CEM, which showed the highest PLK1 expression, high levels were also detected in the EWS cell lines, CADO-ES-1, STA-ET-1 and STA-ET-2.1, the AML cell line, HL-60, the MB cell line, UW228.2, and the NB cell line, IMR-5. The CCRF-CEM cell line with the highest PLK1 expression was also most sensitive to GW843682X. However, although GI_{50s} of GW843682X tended to be lower in cell lines with higher PLK1 expression, no significant associations between the GW843682X-induced growth inhibition (GI_{50s}) or cytotoxicity (LC_{50s}) and PLK1 expression were observed (PLK1 expression vs. $GI_{50-GW843682X}$: $r^2 = -0.460$, $P = 0.055$; PLK1 expression vs. $LC_{50-GW843682X}$: $r^2 = -0.205$, $P = 0.414$) (Pearson product-moment correlation).

Except in the OS cell lines, GW843682X was less toxic than the topoisomerase I inhibitor, CPT. For MNNG-HOS, the GI_{50} of GW843682X was on average about six times lower than the GI_{50} of CPT, whereas the LC_{50} of GW8 43682X was about 10 times lower than the LC_{50} of CPT. GI_{50s} of CPT ranged from 0.003 μmol/l for CCRF-CEM to 7.16 μmol/l for MNNG-HOS. For the leukaemia cell lines and the EWS cell lines, CADO-ES-1 and STA-ET-2.1, the GI_{50s} were below 10 nmol/l. LC_{50s} ranged from 0.008 μmol/l for MOLT-4 to 16.2 μmol/l for MNNG-HOS. With respect to its growth inhibitory effects, four of four leukaemia cell lines, three of four EWS cell lines, two of four NB cell lines and one of two RMS cell lines were sensitive to CPT (Fig. 3a). With regard to the differences of mean calculated for the LC_{50s}, four of four EWS cell lines, two of four leukaemia cell lines, two of four NB cell lines and one of two RMS cell lines were sensitive to CPT (Fig. 3b).

The difference in drug sensitivity/resistance profiles between GW843682X and CPT was also reflected by correlation analysis of toxicity data with ABC-transporter expression (Fig. 4). Gene expression profiling of the ABC transporter *ACCB1*, *ABCC1*, *ABCC2*, *ABCC3*, *ABCC5*, *ABCC6* and *ABCG2* showed no association between the GI_{50s} and LC_{50s} of GW843682X and any of the analysed ABC transporters, whereas the growth inhibitory effects of CPT significantly correlated with the expression of *ABCC1*, *ABCC2* and *ABCC3* (*ABCC1*: $r^2 = 0.640$, $P = 0.004$; *ABCC2*: $r^2 = 0.570$, $P = 0.014$; *ABCC3*: $r^2 = 0.747$, $P = 0.0004$) (Pearson product-moment correlation).

Fig. 1

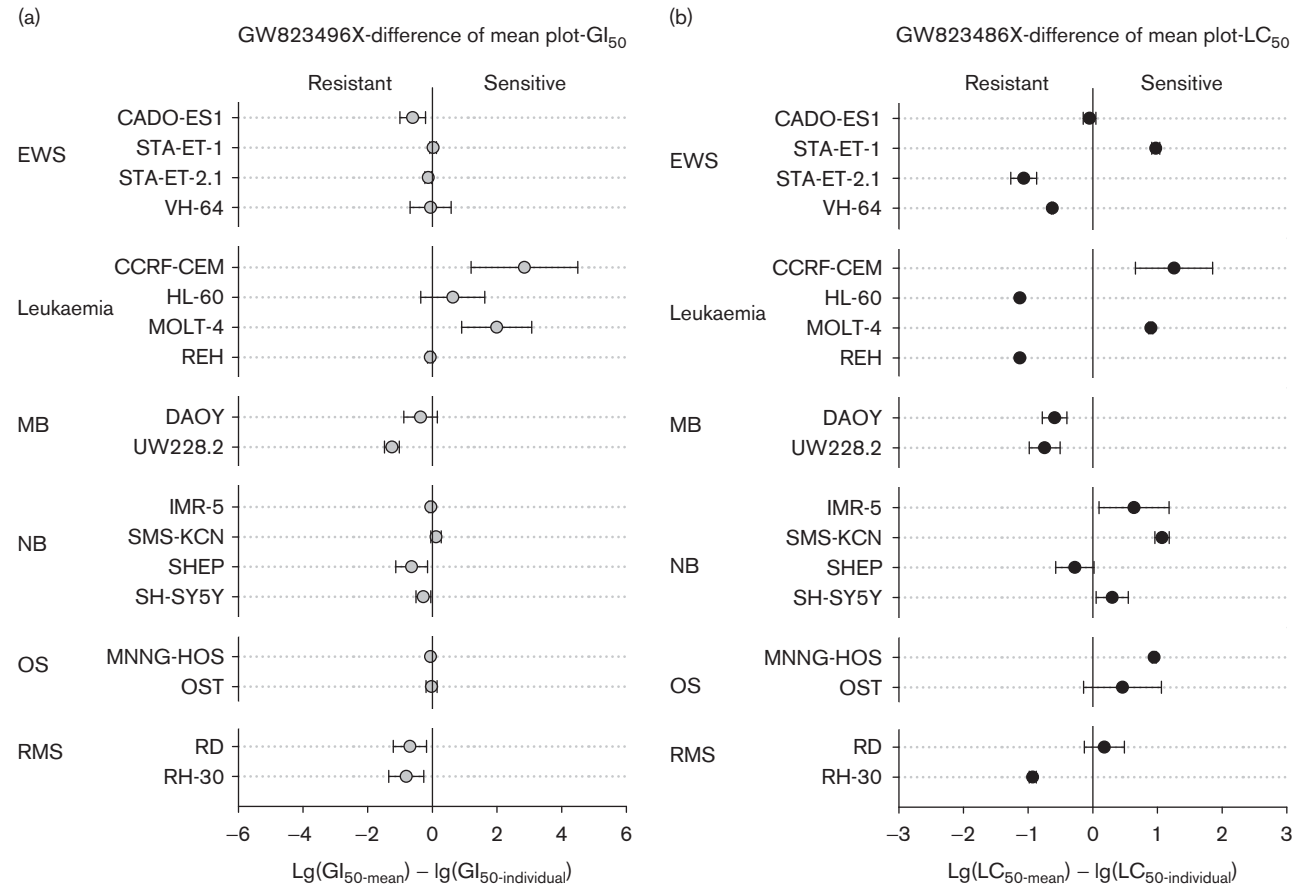

Difference of mean plot on the basis of the half maximal growth inhibitory concentration (GI_{50}) (a) and lethal concentration (LC_{50}) (b) calculated for GW843682X. Mean GI_{50} and LC_{50} were calculated from all experiments and the difference between the mean GI_{50}/LC_{50} and the individual GI_{50}/LC_{50} was calculated. Negative values indicate cell lines that were more resistant (GI_{50s}/LC_{50s} higher than the overall mean). Positive values indicate cell lines that were more sensitive (GI_{50s}/LC_{50s} lower than the overall mean). EWS, Ewing sarcoma; MB, medulloblastoma; NB, neuroblastoma; OS, osteosarcoma; RMS, rhabdomyosarcoma.

Compared with standard anticancer drugs tested on this panel of paediatric tumour cell lines, the sensitivity of the OS cell lines to GW843682X was comparable with their sensitivity to doxorubicin, vincristine, paclitaxel, etoposide, topotecan, cisplatin and carmustine with respect to growth inhibition (GI_{50s}) and was even superior with respect to cytotoxicity (LC_{50}) (Fig. 5). The efficacy of GW843682X against OS cell lines was further confirmed in three additional OS cell lines, namely MG-63, U2OS and SAOS-2 (Fig. 6).

Toxicity of GW843682X was associated with the induction of apoptosis as shown by the measurement of caspase 3/7 activation in the OS cell lines, MNNG-HOS and OST, and in the EWS cell line, STA-ET-1 (Fig. 7).

In 14 out of 16 cell lines, CPT was more cytotoxic than GW843682X. In these cell lines, the combination of CPT and GW843682X in a constant ratio of 1:1 did not influence the growth inhibitory effects of CPT. The dose–response curves of CPT and CPT combined with an equal molar concentration of GW843682X were almost identical (Fig. 8a). Only in the EWS cell line, STA-ET-2.1, the combination of CPT with GW843682X decreased the CPT-induced growth inhibition, whereas it increased the growth inhibitory effects of CPT in the NB cell line, IMR-5 (Fig. 8b and c). In the OS cell lines, which were more sensitive to GW843682X than to CPT, the toxicity of GW843682X was reduced when combined with CPT (Fig. 8d).

Discussion

In search of more selective anticancer drugs, PLK1 emerged as a promising target because it plays a key role in mitotic progression. PLK1 is almost exclusively expressed in proliferating tumour cells and its overexpression in human tumours is associated with poor prognosis [2,3]. Although a few PLK1 inhibitors, such as BI 2536 and BI 6727, have already entered phase 1 clinical trials [7,8], only a little information is available about the use of PLK1 inhibitors against paediatric malignancies. To prove

Fig. 2

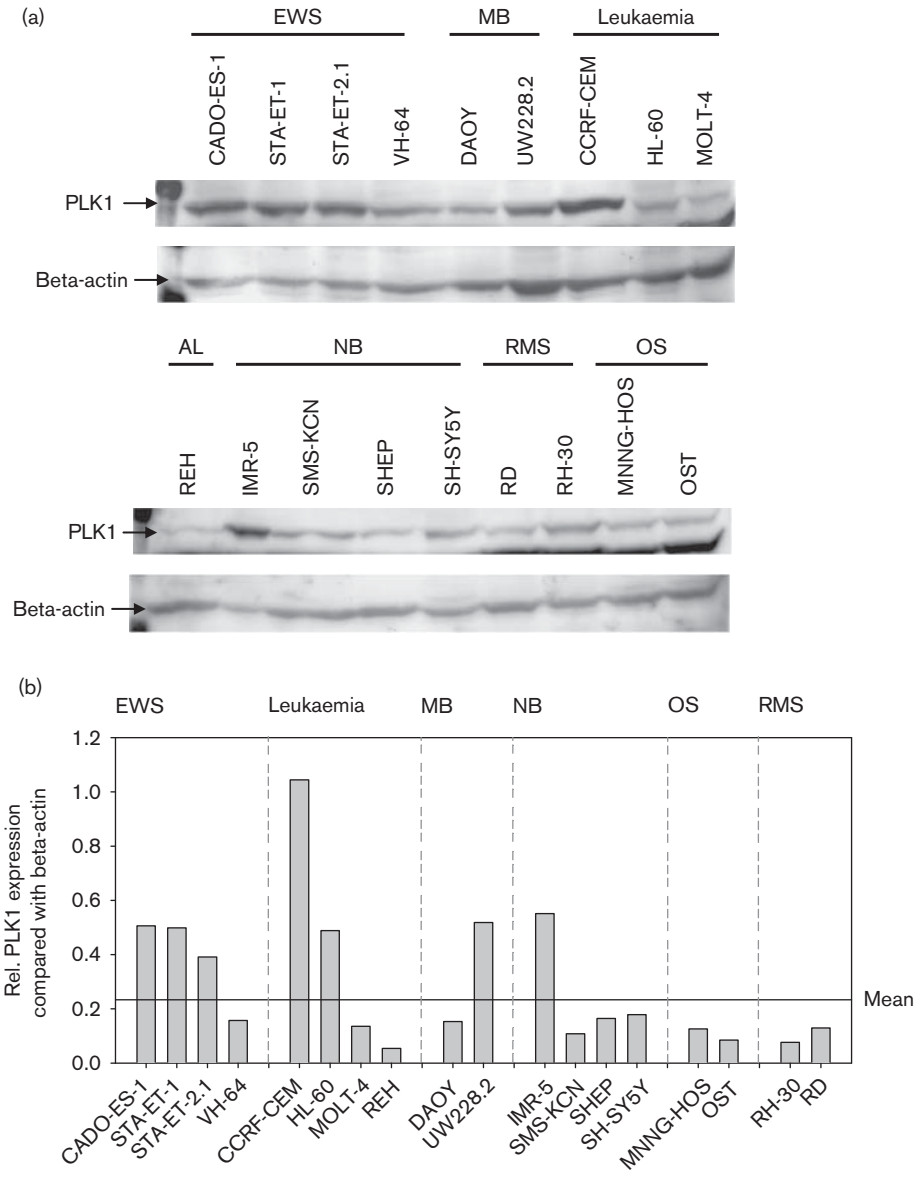

Expression of Polo-like kinase 1 (PLK1) protein in the tumour cell line panel by western blot (a) and relative PLK1 expression compared with beta-actin expression (b). EWS, Ewing sarcoma; MB, medulloblastoma; NB, neuroblastoma; OS, osteosarcoma; RMS, rhabdomyosarcoma.

the concept of PLK1 inhibition by small molecules for the treatment of paediatric malignancies, we evaluated the publicly available PLK1 inhibitor GW843682X against a panel of paediatric tumour cell lines. GW843682X is a thiophene benzimidazole ATP-competitive inhibitor of PLK1. With an half maximal inhibitory concentration (IC_{50}) of 2.2 nmol/l it is among the most potent PLK1 inhibitors [1]. In our panel of 18 cell lines, we determined GI_{50s} for GW863482X in the range of 0.02–11.7 µmol/l, which closely resembled those determined *in vitro* for adult malignancies [56]. Except for the cell lines REH and HL-60, in which LC_{50s} did not reach the highest test concentration of 100 µmol/l, PLK1 inhibition by GW843682X was also cytotoxic with LC_{50s} ranging from 0.64 to 73.0 µmol/l. PLK1 was expressed and, thus, targeted in all cell lines studied. The extent of PLK1 expression varied between the cell lines, and the most sensitive cell line CCRF-CEM was also characterized by the highest expression of PLK1. However, cell lines which were sensitive to GW843682X were not necessarily those with the highest PLK1 expression. This might be attributed to the fact that, in contrast to primary tumours, permanent tumour cell lines ideally proliferate continuously and homogenously *in vitro* and, thus, a part of the cell population *in vitro* is always undergoing mitosis and expresses PLK1 to be targeted by GW843682X. Moreover, apart

Fig. 3

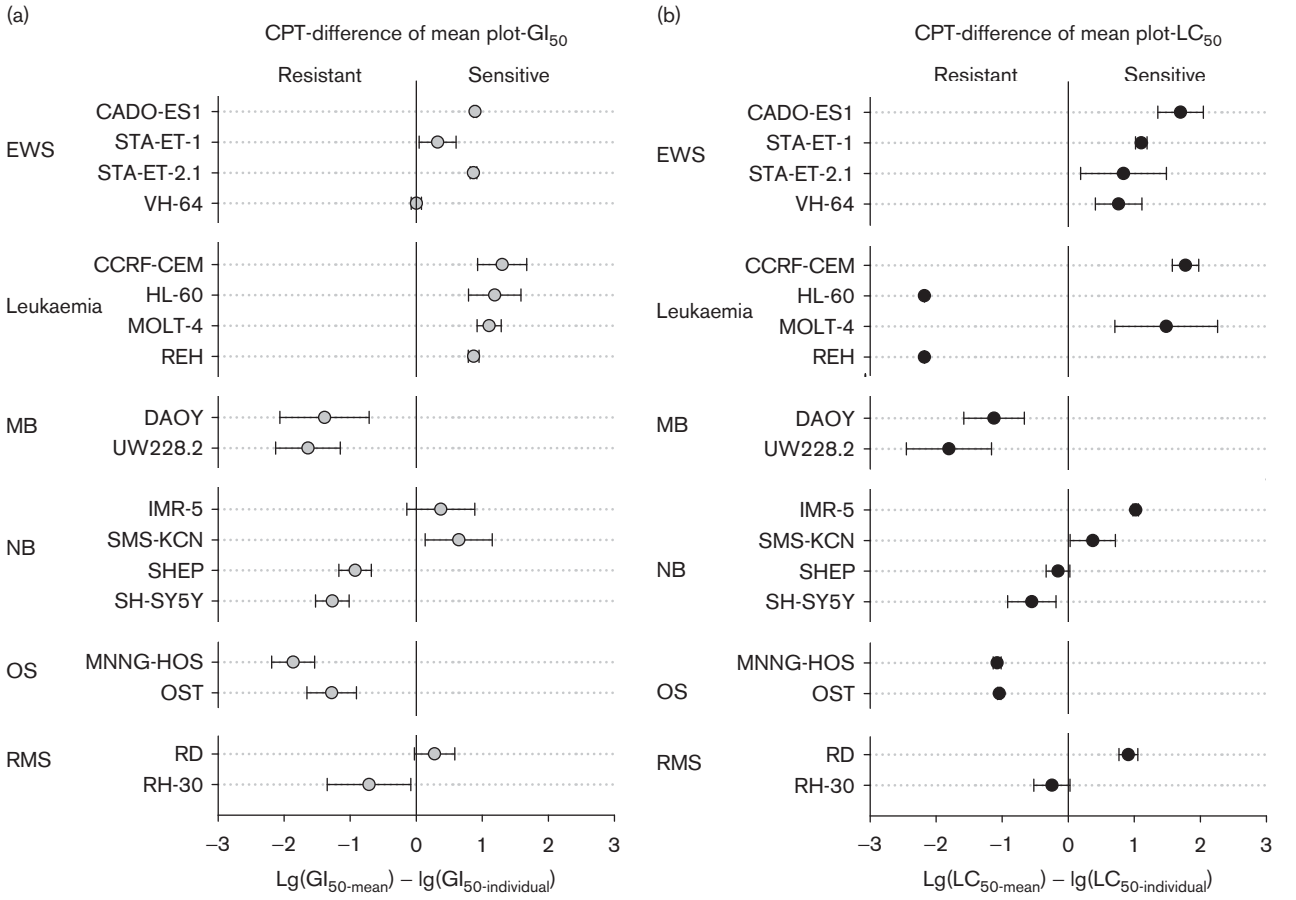

Difference of mean plot on the basis of the half maximal growth inhibitory concentration (GI_{50}) (a) and lethal concentration (LC_{50}) (b) calculated for camptothecin (CPT). Mean GI_{50} and LC_{50} were calculated from all experiments and the difference between the mean GI_{50}/LC_{50} and the individual GI_{50}/LC_{50} was calculated. Negative values indicate cell lines that were more resistant (GI_{50s}/LC_{50s} higher than the overall mean). Positive values indicate cell lines that were more sensitive (GI_{50s}/LC_{50s} lower than the overall mean). EWS, Ewing sarcoma; MB, medulloblastoma; NB, neuroblastoma; OS, osteosarcoma; RMS, rhabdomyosarcoma.

from target gene expression, the efficacy of drugs is additionally determined by their uptake, degradation and/or elimination, which might vary between different cell lines.

With an IC_{50} of 2.2 nmol/l for PLK1, GW843682X was more than 100-fold selective over 30 other kinases including the cyclin-dependent kinases cdk1 and cdk2, but it was only approximately four-fold more selective over PLK3 [56]. The family of PLKs is highly conserved, and so far all ATP-competitive PLK1 inhibitors also target, to varying extents, other members of the PLK family, that is, PLK2 and PLK3 [1]. Although PLK1 regulates mitosis, PLK2 and PLK3 were reported to mediate p53-dependent stress response of cancer cells to DNA damage and oxidative stress [57–59]. Inhibition of PLK2 and PLK3 might, therefore, compromise the p53-mediated stress response to DNA-damaging anticancer drugs such as the topoisomerase inhibitor, CPT. As the GI_{50s} and LC_{50s} of GW843682X were above its IC_{50} for PLK3 (9.1 nmol/l), PLK1, PLK2 and PLK3 were supposed to be targeted. However, GW843682X combined with CPT at a molar ratio of 1 : 1 did not diminish the toxicity of CPT in 17 out of 18 cell lines, which is in accordance with recently published data, where no additive effects were observed for GW843682X and etoposide in AML cell lines [60]. Moreover, selective knockdown of PLK1 in human cancer cell lines was reported to induce apoptosis independent of mutated p53 [8,61]. For 17 cell lines of our cell line panel, information about p53 mutations was available (Table 1). No significant association between p53 mutations and sensitivity to GW843682X was detected (wild type/mutated p53 vs. $GI_{50-GW843682X}$: $r^2 = 0.024$, $P = 0.021$; wild type/mutated p53 vs. $LC_{50-GW843682X}$: $r^2 = -0.289$, $P = 0.254$) (Spearman rank-order correlation). This suggests that the cytotoxicity of PLK1 inhibition is affected neither by the mutant nor by the inhibited p53 signalling.

Fig. 4

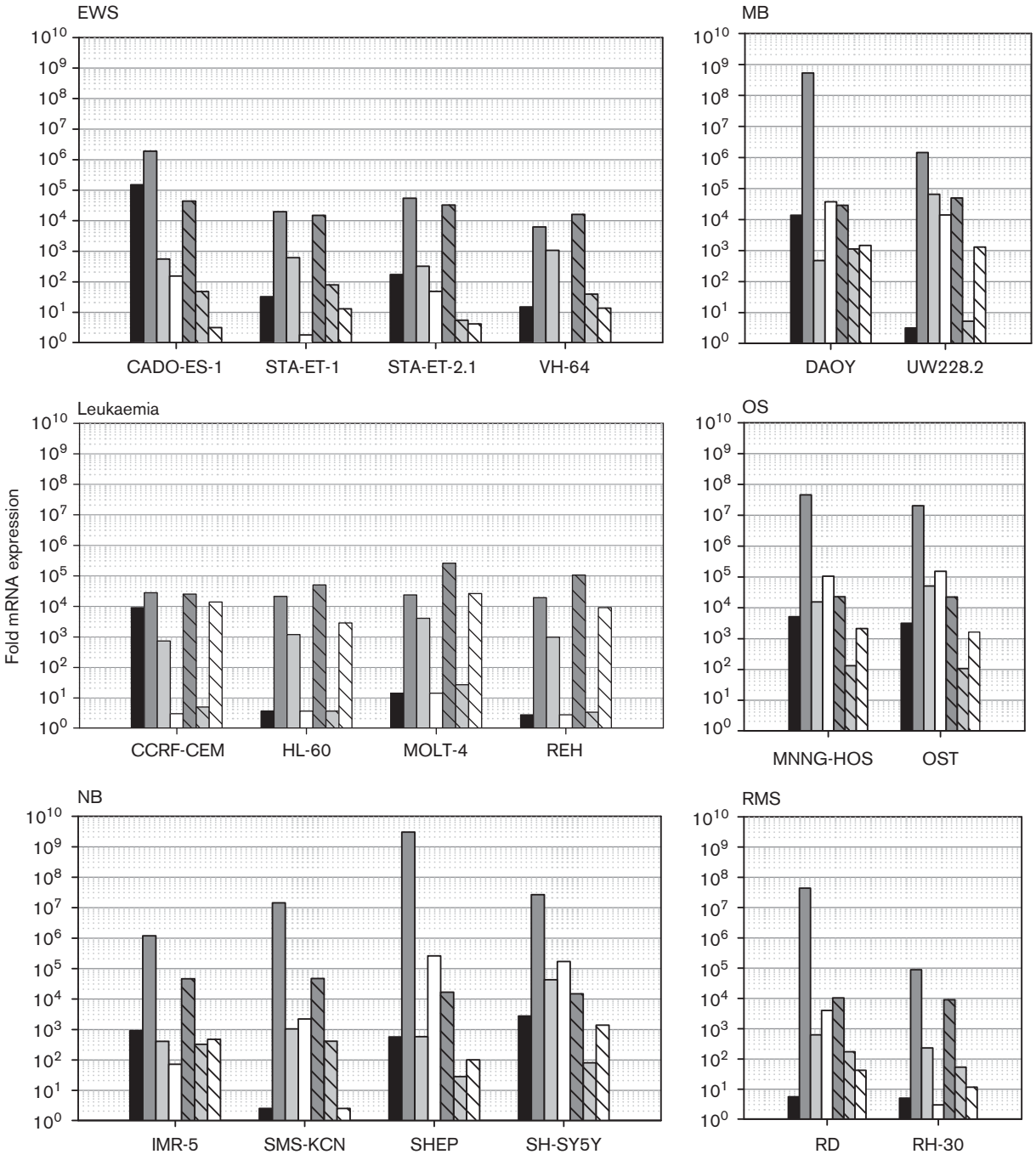

Relative mRNA expression levels of *ABCB1* (■), *ABCC1* (▒), *ABCC2* (▒), *ABCC3* (□), *ABCC5* (▒), *ABCC6* (▒) and *ABCG2* (▒). EWS, Ewing sarcoma; MB, medulloblastoma; NB, neuroblastoma; OS, osteosarcoma; RMS, rhabdomyosarcoma.

Among the NB cell lines that were considered sensitive, two cell lines stemmed from N-Myc-amplified tumours indicating GW843682X activity also to be against these more aggressively growing NBs [62]. Within the cell line panel studied, the OS cell lines, MNNG-HOS and OST, were among the cell lines most resistant to standard anticancer drugs such as doxorubicin, etoposide, cisplatin or carmustine. Therefore, their sensitivity to the cytotoxicity of GW843682X was remarkable (Fig. 4). Their LC_{50} values of GW843682X were approximately 20-fold below those determined for CPT. For all other cell lines, GW843682X was less cytotoxic than CPT. However, apart from its toxicity against tumour cells, the clinical efficacy of an anticancer drug finally also depends on its

Fig. 5

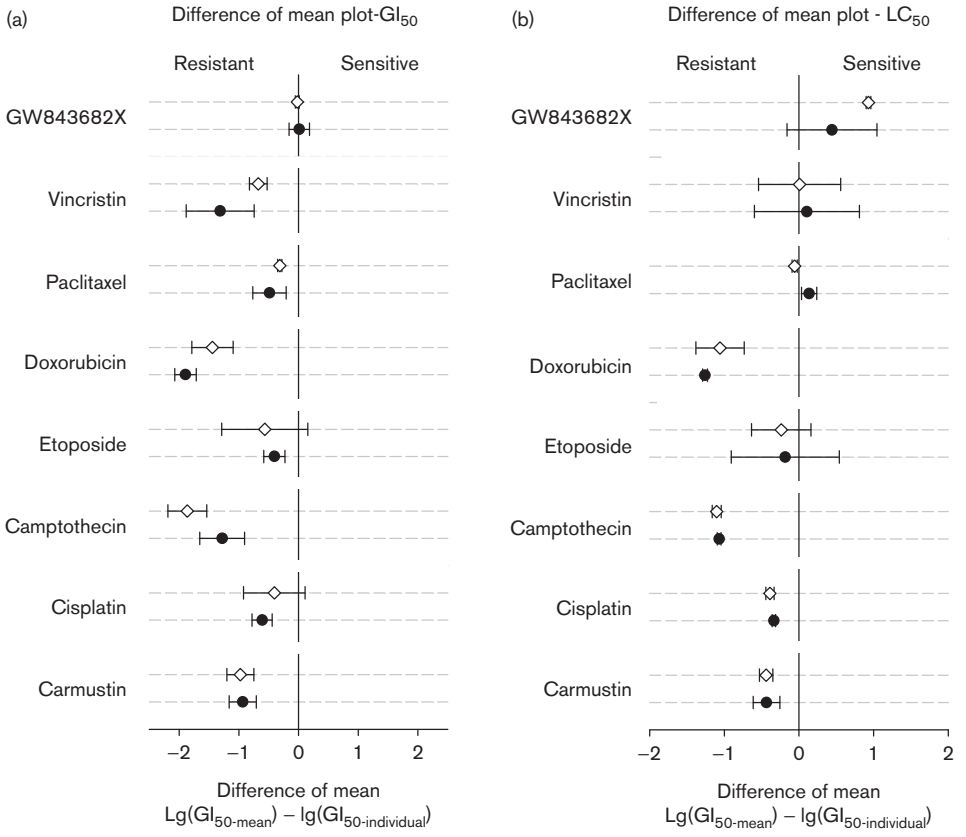

Drug sensitivity/resistance profiles of the osteosarcoma cell lines, MNNG-HOS and OST, to GW843682X and standard anticancer drugs. Mean half maximal growth inhibitory concentration (GI_{50}) and lethal concentration (LC_{50}) were calculated for each drug from all experiments with all 18 cell lines of the panel. The difference between the mean GI_{50}/LC_{50} and the individual GI_{50}/LC_{50} was calculated individually for each drug and these differences were compiled for MNNG-HOS (-◇-) and OST (-●-) according to GI_{50s} (a) and LC_{50s} (b). Positive values indicate a more sensitive phenotype [$lg(GI_{50})/lg(LC_{50})$ lower compared with the overall mean].

Fig. 6

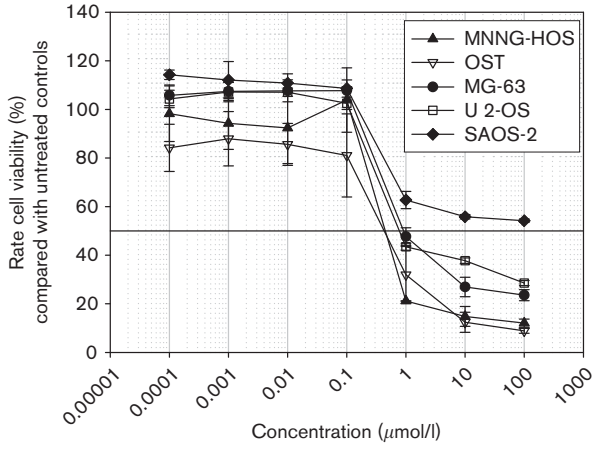

Dose-dependent growth inhibition of GW843682X for osteosarcoma cell lines, MNNG-HOS (-▲-), OST (-▽-), MG-63 (-●-), U2-OS (-□-) and SAOS-2 (-◆-). The reference line represents 50% reduction of cell viability compared with untreated controls.

Fig. 7

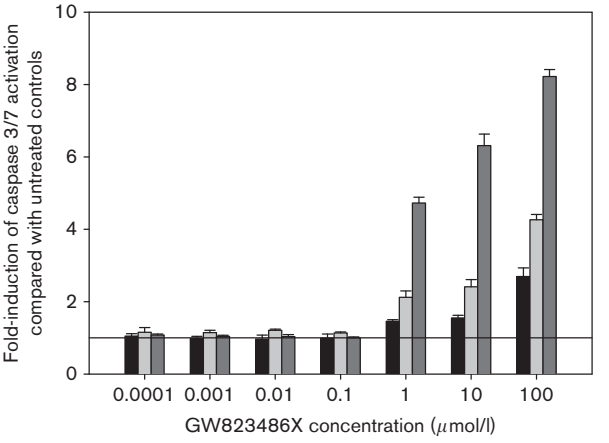

Activation of caspase 3/7 by GW843682X in the osteosarcoma cell lines, MNNG-HOS ( ) and OST ( ), and the Ewing sarcoma cell line, STA-ET-1, ( ). Cells were exposed to increasing concentrations of GW843682X for 24 h.

Fig. 8

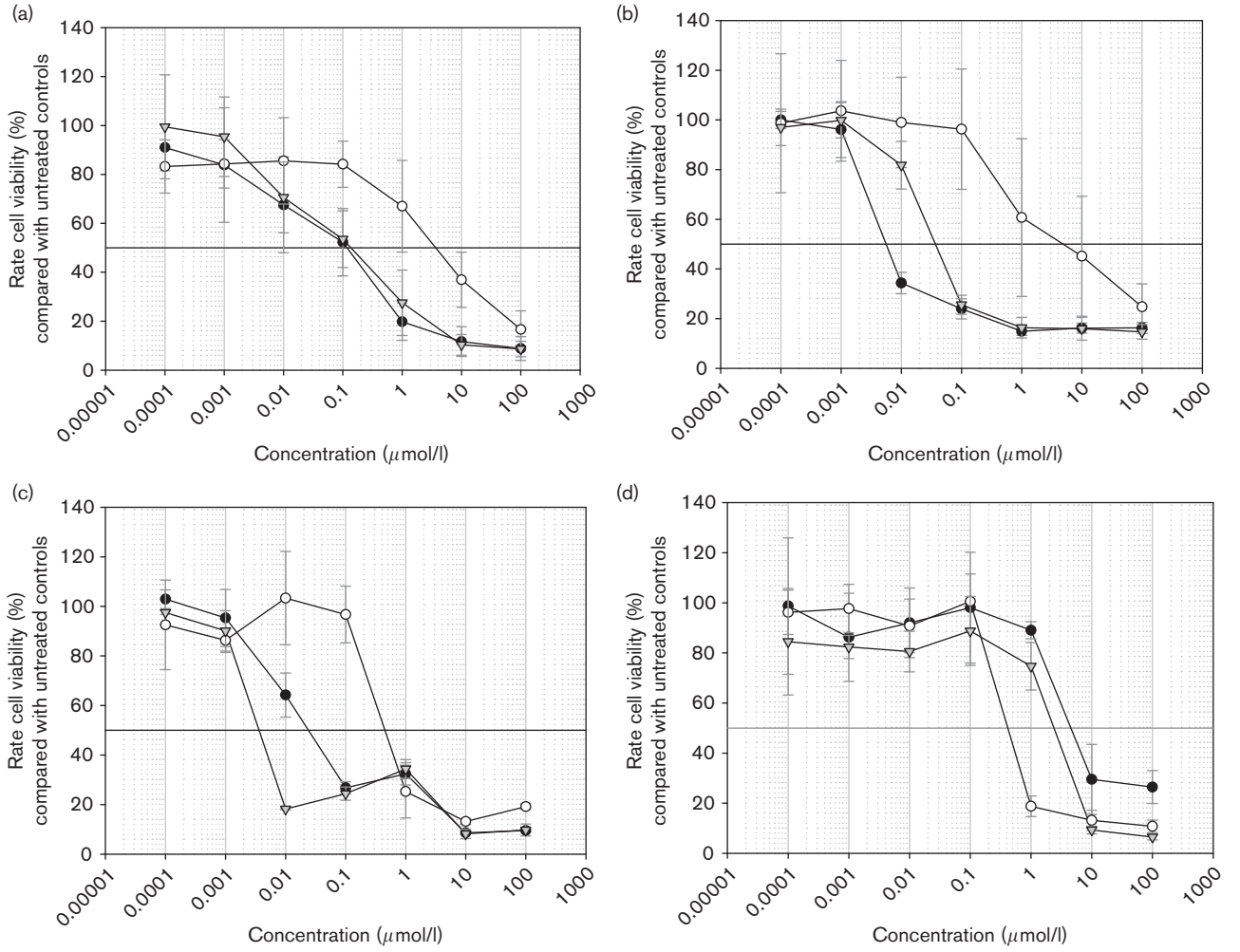

Mean dose–response curves of camptothecin (CPT) (-●-), GW843682X (-○-) and CPT combined with GW843682X (—▽—) at equimolar concentrations determined from three individual experiments for the rhabdomyosarcoma cell line, RH-30, (a), the Ewing sarcoma cell line, STA-ET-2.1, (b), the neuroblastoma cell line, IMR-5, (c) and the osteosarcoma cell line, MNNG-HOS, (d). The reference line represents 50% reduction of cell viability compared with untreated controls.

tolerability; the molar GI_{50s} and LC_{50s} of different drugs are less meaningful unless their tolerability is known. In this respect, PLK1 inhibitors are especially promising, as it was shown that they, at least *in vitro*, did not affect nonmalignant cells [6]. More significant are the different sensitivity and resistance profiles of GW843682X and CPT as depicted in their difference of mean plots indicating activity of GW843682X against CPT-resistant tumours. GW843682X was obviously no substrate for ABC transporters, because in contrast to CPT its toxicity was not inversely associated with the expression of ABC transporters. For the PLK1 inhibitor BI 6727, comparable observations were made, as it was cytotoxic against a taxane-resistant colorectal cancer cell line expressing high levels of ABCB2 [63]. Expression of ABC transporters is one main reason for intrinsic and acquired resistance of many tumours against numerous standard anticancer drugs [64]. New drugs, which are no substrates for these transporters, offer, apart from their new mechanism of action, additional advantages, especially for patients with advanced, progressive or relapsed diseases who failed to respond to standard treatment.

In this study, we also addressed concomitant combination testing of GW843682X with the topoisomerase 1 inhibitor, CPT, at equimolar concentrations and found no interference between CPT and GW843682X with respect to growth inhibition in the majority of cell lines. Antagonism of GW843682X effects by CPT was observed for the GW843682X-sensitive OS cell lines. Antagonism of CPT toxicity by GW843682X on the one hand and synergy between CPT and GW843682X on the other were observed only for the EWS, STA-ET-2.1, and the NB cell lines, IMR-5, respectively. The fact that this preliminary

combination screen per se revealed no antagonistic effects between GW843682X and the cytotoxic topoisomerase I inhibitor CPT in the majority of cell lines renders the integration of PLK1 inhibition in combinatorial drug therapy possible. Combinations of PLK1 inhibitors with other anticancer drugs and different exposure sequences might well detect more significant synergies between PLK1 inhibition and other anticancer drugs.

We successfully tested the in-vitro toxicity of the publicly available PLK1 inhibitor GW843682X against a panel of paediatric tumour cell lines. Especially two OS cell lines highly resistant to almost all standard anticancer drugs responded well, as well as two NB cell lines, which were derived from tumours with unfavourable prognosis. The PLK1 inhibitor BI 2536 has already entered clinical trials and was reported to induce disease stabilization while being well-tolerated [8]. Other PLK1 inhibitors such as BI 6727 are under clinical development. These inhibitors have an even higher affinity for PLK1 and are even more selective over PLK2 and PLK3. Our results strongly suggest that these drugs should be evaluated against paediatric malignancies to allow a timely access to these promising anticancer drugs in children in the same way as that of adults.

Acknowledgements

The authors thank S. Hoogestraat, S. Schulz and P. Schulze Westhoff for their excellent technical assistance. This study was supported by the Federal Department of Research and Technology (01EC9801) and by 'Horizont' Kinderkrebshilfe Weseke e.V. This study fulfills the requirements for the medical doctoral thesis of K.S.

References

1 Strebhardt K, Ullrich A. Targeting polo-like kinase 1 for cancer therapy. *Nat Rev Cancer* 2006; **6**:321–330.
2 Barr FA, Silljé HH, Nigg EA. Polo-like kinases and the orchestration of cell division. *Nat Rev Mol Cell Biol* 2004; **5**:429–440.
3 Takai N, Hamanaka R, Yoshimatsu J, Miyakawa I. Polo-like kinases (Plks) and cancer. *Oncogene* 2005; **24**:287–291.
4 Yim H, Erikson RL. Polo-like kinase 1 depletion induces DNA damage in early S prior to caspase activation. *Mol Cell Biol* 2009; **29**:2609–2621.
5 Bu Y, Yang Z, Li Q, Song F. Silencing of polo-like kinase (Plk) 1 via siRNA causes inhibition of growth and induction of apoptosis in human esophageal cancer cells. *Oncology* 2008; **74**:198–206.
6 Liu X, Lei M, Erikson RL. Normal cells, but not cancer cells, survive severe Plk1 depletion. *Mol Cell Biol* 2006; **26**:2093–2108.
7 Steegmaier M, Hoffmann M, Baum A, Lénárt P, Petronczki M, Krssák M, *et al.* BI 2536, a potent and selective inhibitor of polo-like kinase 1, inhibits tumor growth *in vivo*. *Curr Biol* 2007; **17**:316–322.
8 Mross K, Frost A, Steinbild S, Hedbom S, Rentschler J, Kaiser R, *et al.* Phase I dose escalation and pharmacokinetic study of BI 2536, a novel Polo-like kinase 1 inhibitor, in patients with advanced solid tumors. *J Clin Oncol* 2008; **26**:5511–5517.
9 Hu K, Lee C, Qiu D, Fotovati A, Davies A, Abu-Ali S, *et al.* Small interfering RNA library screen of human kinases and phosphatases identifies polo-like kinase 1 as a promising new target for the treatment of pediatric rhabdomyosarcomas. *Mol Cancer Ther* 2009; **8**:3024–3035.
10 Kodama K, Doi O, Higashiyama M, Mori Y, Horai T, Tateishi R, *et al.* Establishment and characterization of a new Ewing's sarcoma cell line. *Cancer Genet Cytogenet* 1991; **57**:19–30.
11 Kodama K, Doi O, Higashiyama M, Yokouchi H, Tateishi R, Mori Y. Differentiation of a Ewing's sarcoma cell line towards neural and mesenchymal cell lineages. *Jpn J Cancer Res* 1994; **85**:335–338.
12 Ottaviano L, Schaefer KL, Gajewski M, Huckenbeck W, Baldus S, Rogel U, *et al.* Molecular characterization of commonly used cell lines for bone tumor research: a trans-European EuroBoNet effort. *Genes Chromosomes Cancer* 2010; **49**:40–51.
13 Ambros IM, Ambros PF, Strehl S, Kovar H, Gadner H, Salzer-Kuntschik M. MIC2 is a specific marker for Ewing's sarcoma and peripheral primitive neuroectodermal tumors. Evidence for a common histogenesis of Ewing's sarcoma and peripheral primitive neuroectodermal tumors from MIC2 expression and specific chromosome aberration. *Cancer* 1991; **67**:1886–1893.
14 Van Valen F, Winkelmann W, Jürgens H. Type I and type II insulin-like growth factor receptors and their function in human Ewing's sarcoma cells. *J Cancer Res Clin Oncol* 1992; **118**:269–275.
15 Foley GE, Lazarus H, Farber S, Uzman BG, Boone BA, McCarthy RE. Continuous culture of human lymphoblasts from peripheral blood of a child with acute leukemia. *Cancer* 1965; **18**:522–529.
16 McCarthy RE, Junius V, Farber S, Lazarus H, Foley GE. Cytogenetic analysis of human lymphoblasts in continuous culture. *Exp Cell Res* 1965; **40**:197–200.
17 Cinti C, Claudio PP, Luca AD, Cuccurese M, Howard CM, D'Esposito M, *et al.* A serine 37 mutation associated with two missense mutations at highly conserved regions of p53 affect pro-apoptotic genes expression in a T-lymphoblastoid drug resistant cell line. *Oncogene* 2000; **19**:5098–5105.
18 Aldridge DR, Radford IR. Explaining differences in sensitivity to killing by ionizing radiation between human lymphoid cell lines. *Cancer Res* 1998; **58**:2817–2824.
19 Collins SJ, Gallo RC, Gallagher RE. Continuous growth and differentiation of human myeloid leukaemic cells in suspension culture. *Nature* 1977; **270**:347–349.
20 Gallagher R, Collins S, Trujillo J, McCredie K, Ahearn M, Tsai S, *et al.* Characterization of the continuous, differentiating myeloid cell line (HL-60) from a patient with acute promyelocytic leukemia. *Blood* 1979; **54**:713–733.
21 Collins SJ. The HL-60 promyelocytic leukemia cell line: proliferation, differentiation, and cellular oncogene expression. *Blood* 1987; **70**:1233–1244.
22 Wolf D, Rotter V. Major deletions in the gene encoding the p53 tumor antigen cause lack of p53 expression in HL-60 cells. *Proc Natl Acad Sci U S A* 1985; **82**:790–794.
23 Minowada J, Onuma T, Moore GE. Rosette-forming human lymphoid cell lines. I. Establishment and evidence for origin of thymus-derived lymphocytes. *J Natl Cancer Inst* 1972; **49**:891–895.
24 Chow VT, Quek HH, Tock EP. Alternative splicing of the p53 tumor suppressor gene in the Molt-4 T-lymphoblastic leukemia cell line. *Cancer Lett* 1993; **73**:141–148.
25 Rosenfeld C, Goutner A, Choquet C, Venuat AM, Kayibanda B, Pico JL, *et al.* Phenotypic characterisation of a unique non-T, non-B acute lymphoblastic leukaemia cell line. *Nature* 1977; **267**:841–843.
26 He XM, Ostrowski LE, Von Wronski MA, Friedman HS, Wikstrand CJ, Bigner SH, *et al.* Expression of O6-methylguanine-DNA methyltransferase in six human medulloblastoma cell lines. *Cancer Res* 1992; **52**:1144–1148.
27 He XM, Skapek SX, Wikstrand CJ, Friedman HS, Trojanowski JQ, Kemshead JT, *et al.* Phenotypic analysis of four human medulloblastoma cell lines and transplantable xenografts. *J Neuropathol Exp Neurol* 1989; **48**:48–68.
28 Portwine C, Chilton-MacNeill S, Brown C, Sexsmith E, McLaughlin J, Malkin D. Absence of germline and somatic p53 alterations in children with sporadic brain tumors. *J Neurooncol* 2001; **52**:227–235.
29 Raffel C, Thomas GA, Tishler DM, Lassoff S, Allen JC. Absence of p53 mutations in childhood central nervous system primitive neuroectodermal tumors. *Neurosurgery* 1993; **33**:301–306.
30 Keles GE, Berger MS, Srinivasan J, Kolstoe DD, Bobola MS, Silber JR. Establishment and characterization of four human medulloblastoma-derived cell lines. *Oncol Res* 1995; **7**:493–503.
31 Pastuszko A, Yee DK, Nelson D, Wilson DF.Calcium dependent regulation of catecholamine and serotonin metabolism in human neuroblastoma cells. *Cancer Biochem Biophys* 1988; **10**:67–76.
32 Kovacina KS, Roth RA. Characterization of the endogenous insulin receptor-related receptor in neuroblastomas. *J Biol Chem* 1995; **270**:1881–1887.
33 Fischer M, Berthold F. Characterization of the gene expression profile of neuroblastoma cell line IMR-5 using serial analysis of gene expression. *Cancer Lett* 2003; **190**:79–87.

34 Torres J, Regan PL, Edo R, Leonhardt P, Jeng EI, Rappaport EF, *et al.* Biological effects of induced MYCN hyper-expression in MYCN-amplified neuroblastomas. *Int J Oncol* 2010; **37**:983–991.

35 Reynolds CP, Biedler JL, Spengler BA, Reynolds DA, Ross RA, Frenkel EP, *et al.* Characterization of human neuroblastoma cell lines established before and after therapy. *J Natl Cancer Inst* 1986; **76**:375–387.

36 Keshelava N, Zuo JJ, Chen P, Waidyaratne SN, Luna MC, Gomer CJ, *et al.* Loss of p53 function confers high-level multidrug resistance in neuroblastoma cell lines. *Cancer Res* 2001; **61**:6185–6193.

37 Spengler BA, Biedler JL, Ross RA. A corrected karyotype for the SH-SY5Y human neuroblastoma cell line. *Cancer Genet Cytogenet* 2002; **138**:177–178.

38 Ross RA, Spengler BA, Biedler JL. Coordinate morphological and biochemical interconversion of human neuroblastoma cells. *J Natl Cancer Inst* 1983; **71**:741–747.

39 Sadée W, Yu VC, Richards ML, Preis PN, Schwab MR, Brodsky FM, *et al.* Expression of neurotransmitter receptors and myc protooncogenes in subclones of a human neuroblastoma cell line. *Cancer Res* 1987; **47**:5207–5212.

40 Tweddle DA, Malcolm AJ, Cole M, Pearson AD, Lunec J. p53 cellular localization and function in neuroblastoma: evidence for defective G(1) arrest despite WAF1 induction in MYCN-amplified cells. *Am J Pathol* 2001; **158**:2067–2077.

41 Carr J, Bell E, Pearson AD, Kees UR, Beris H, Lunec J, *et al.* Increased frequency of aberrations in the p53/MDM2/p14(ARF) pathway in neuroblastoma cell lines established at relapse. *Cancer Res* 2006; **66**:2138–2145.

42 Goldstein D, Leavitt J. Expression of neoplasia-related proteins of chemically transformed HuT fibroblasts in human osteosarcoma HOS fibroblasts and modulation of actin expression upon elevation of tumorigenic potential. *Cancer Res* 1985; **45**:3256–3261.

43 Park M, Testa JR, Blair DG, Parsa NZ, Vande Woude GF. Two rearranged MET alleles in MNNG-HOS cells reveal the orientation of MET on chromosome 7 to other markers tightly linked to the cystic fibrosis locus. *Proc Natl Acad Sci U S A* 1988; **85**:2667–2671.

44 Roepke M, Diestel A, Bajbouj K, Walluscheck D, Schonfeld P, Roessner A, *et al.* Lack of p53 augments thymoquinone-induced apoptosis and caspase activation in human osteosarcoma cells. *Cancer Biol Ther* 2007; **6**:160–169.

45 Tomita K, Tsuchiya H. Enhancement of cytocidal and antitumor effect of cisplatin by caffeine in human osteosarcoma. *Clin Ther* 1989; **11**:43–52.

46 Tomita K, Kontani T, Tsuchiya H, Nomura S. Drug resistance and cross-sensitivity in cultured human osteosarcoma cells. *Nippon Seikeigeka Gakkai Zasshi* 1989; **63**:274–281.

47 Asada N, Tsuchiya H, Tomita K. De novo deletions of p53 gene and wild-type p53 correlate with acquired cisplatin-resistance in human osteosarcoma OST cell line. *Anticancer Res* 1999; **19**:5131–5137.

48 McAllister RM, Melnyk J, Finkelstein JZ, Adams EC Jr, Gardner MB. Cultivation in vitro of cells derived from a human rhabdomyosarcoma. *Cancer* 1969; **24**:520–526.

49 Chen TR, Dorotinsky C, Macy M, Hay R. Cell identity resolved. *Nature* 1989; **340**:106.

50 Gershwin ME, Ikeda RM, Kawakami TG, Owens RB. Immunobiology of heterotransplanted human tumors in nude mice. *J Natl Cancer Inst* 1977; **58**:1455–1461.

51 Felix CA, Kappel CC, Mitsudomi T, Nau MM, Tsokos M, Crouch GD, *et al.* Frequency and diversity of p53 mutations in childhood rhabdomyosarcoma. *Cancer Res* 1992; **52**:2243–2247.

52 Douglass EC, Valentine M, Etcubanas E, Parham D, Webber BL, Houghton PJ, *et al.* A specific chromosomal abnormality in rhabdomyosarcoma. *Cytogenet Cell Genet* 1987; **45**:148–155.

53 Gibson AA, Harwood FG, Tillman DM, Houghton JA. Selective sensitization to DNA-damaging agents in a human rhabdomyosarcoma cell line with inducible wild-type p53 overexpression. *Clin Cancer Res* 1998; **4**:145–152.

54 Taylor AC, Shu L, Danks MK, Poquette CA, Shetty S, Thayer MJ, *et al.* P53 mutation and MDM2 amplification frequency in pediatric rhabdomyosarcoma tumors and cell lines. *Med Pediatr Oncol* 2000; **35**:96–103.

55 Lanvers-Kaminsky C, Bremer A, Dirksen U, Jürgens H, Boos J. Cytotoxicity of treosulfan and busulfan on pediatric tumor cell lines. *Anticancer Drugs* 2006; **17**:657–662.

56 Lansing TJ, McConnell RT, Duckett DR, Spehar GM, Knick VB, Hassler DF, *et al.* In vitro biological activity of a novel small-molecule inhibitor of polo-like kinase 1. *Mol Cancer Ther* 2007; **6**:450–459.

57 Yang Y, Bai J, Shen R, Brown SA, Komissarova E, Huang Y, *et al.* Polo-like kinase 3 functions as a tumor suppressor and is a negative regulator of hypoxia-inducible factor-1 alpha under hypoxic conditions. *Cancer Res* 2008; **68**:4077–4085.

58 Wang L, Gao J, Dai W, Lu L. Activation of Polo-like kinase 3 by hypoxic stresses. *J Biol Chem* 2008; **283**:25928–25935.

59 Matthew EM, Hart LS, Astrinidis A, Navaraj A, Dolloff NG, Dicker DT, *et al.* The p53 target Plk2 interacts with TSC proteins impacting mTOR signaling, tumor growth and chemosensitivity under hypoxic conditions. *Cell Cycle* 2009; **8**:4168–4175.

60 Didier C, Cavelier C, Quaranta M, Demur C, Ducommun B. Evaluation of Polo-like Kinase 1 inhibition on the G2/M checkpoint in Acute Myelocytic Leukaemia. *Eur J Pharmacol* 2008; **591**:102–105.

61 Guan R, Tapang P, Leverson JD, Albert D, Giranda VL, Luo Y. Small interfering RNA-mediated Polo-like kinase 1 depletion preferentially reduces the survival of p53-defective, oncogenic transformed cells and inhibits tumor growth in animals. *Cancer Res* 2005; **65**:2698–2704.

62 Schwab M. Amplification of N-myc as a prognostic marker for patients with neuroblastoma. *Semin Cancer Biol* 1993; **4**:13–18.

63 Rudolph D, Steegmaier M, Hoffmann M, Grauert M, Baum A, Quant J, *et al.* BI 6727, A polo-like kinase inhibitor with improved pharmacokinetic profile and broad antitumor activity. *Clin Cancer Res* 2009; **15**:3094–3102.

64 Gottesman MM. Mechanisms of cancer drug resistance. *Annu Rev Med* 2002; **53**:615–627.